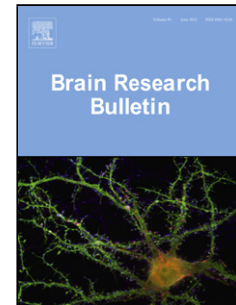


Accepted Manuscript

Title: SLEEP DISORDER AND ALTERED LOCOMOTOR ACTIVITY AS BIOMARKERS OF THE PARKINSON'S DISEASE CHOLINOPATHY IN RAT

Authors: Jelena Ciric, Katarina Lazic, Slobodan Kapor, Milka Perovic, Jelena Petrovic, Vesna Pesic, Selma Kanazir, Jasna Saponjic



PII: S0166-4328(17)31239-1
DOI: <https://doi.org/10.1016/j.bbr.2017.11.021>
Reference: BBR 11180

To appear in: *Behavioural Brain Research*

Received date: 27-7-2017
Revised date: 7-9-2017
Accepted date: 16-11-2017

Please cite this article as: Ciric Jelena, Lazic Katarina, Kapor Slobodan, Perovic Milka, Petrovic Jelena, Pesic Vesna, Kanazir Selma, Saponjic Jasna. SLEEP DISORDER AND ALTERED LOCOMOTOR ACTIVITY AS BIOMARKERS OF THE PARKINSON'S DISEASE CHOLINOPATHY IN RAT. *Behavioural Brain Research* <https://doi.org/10.1016/j.bbr.2017.11.021>

This is a PDF file of an unedited manuscript that has been accepted for publication. As a service to our customers we are providing this early version of the manuscript. The manuscript will undergo copyediting, typesetting, and review of the resulting proof before it is published in its final form. Please note that during the production process errors may be discovered which could affect the content, and all legal disclaimers that apply to the journal pertain.

SLEEP DISORDER AND ALTERED LOCOMOTOR ACTIVITY AS BIOMARKERS OF THE PARKINSON'S DISEASE CHOLINOPATHY IN RAT

Running title: Biomarkers of Parkinson's disease cholinopathy in rat

Jelena Ciric^a, Katarina Lazic^a, Slobodan Kapor^{a,b}, Milka Perovic^a, Jelena Petrovic^a, Vesna Pestic^a, Selma Kanazir^a, Jasna Saponjic^{a,*}

^aUniversity of Belgrade, Department of Neurobiology, Institute for Biological Research - Sinisa Stankovic,

^bUniversity of Belgrade, Medical School, Belgrade, Serbia.

*Corresponding author

Jasna Saponjic, M.D., Ph.D. Research Professor University of Belgrade, Department of Neurobiology, Institute for Biological Research-Sinisa Stankovic, Despot Stefan Blvd. 142, 11060 Belgrade, Serbia Phone: + 381 11 2078426, Fax: + 381 11 2761433, e-mail: jasnasap@ibiss.bg.ac.rs, jasnasaponjic@yahoo.com

Highlights

- Hippocampal sleep disorder is the first and long-lasting hallmark of PD cholinopathy.
- High voltage sleep spindle dynamics during REM sleep reflects PD cholinopathy.
- Hypokinesia reflects impaired cholinergic impact in motor control regulatory network.
- Amphetamine induces hyperactivity in the hypokinetic rats with PD cholinopathy.
- Putamen c-Fos activity reflects re-organization of motor control in PD cholinopathy.

Abstract

In order to find out the possible earliest biomarkers of Parkinson's disease (PD) cholinopathy, we followed the impact of bilateral pedunculopontine tegmental nucleus (PPT)

lesion in rat on: the cortical and hippocampal sleep/wake states architectures, all sleep states related EEG microstructures, sleep spindles, the basal and stimulated locomotor activity.

Sleep and basal locomotor activity in adult Wistar rats were followed during their inactive circadian phase, and throughout the same aging period. The bilateral PPT lesions were done by 0.1 M ibotenic acid (IBO) during the surgical procedure for implantation of the electroencephalographic (EEG) and electromyographic (EMG) electrodes for chronic sleep recording. The cholinergic neuronal loss was identified by NADPH - diaphorase histochemistry. After all sleep and behavioral recording sessions, the locomotor activity was stimulated by d-amphetamine (d-AMPH) and the neuronal activity of striatum was followed by c-Fos immunolabeling.

Impaired cholinergic innervation from the PPT was expressed earlier as sleep disorder than as movement disorder, and it was the earliest and long-lasting at hippocampal and thalamo-cortical level, and followed by a delayed “hypokinesia”. This severe impact of a tonically impaired PPT cholinergic innervation was evidenced as the cholinergic interneuronal loss of the caudate putamen and as a suppressed c-Fos expression after stimulation by d-AMPH.

In order how they occurred, the hippocampal non rapid eye movement (NREM) sleep disorder, altered high voltage sleep spindle (HVS) dynamics during rapid eye movement (REM) sleep in the hippocampus and motor cortex, and „hypokinesia” may serve as the biomarkers of PD cholinopathy onset and progression.

List of abbreviations:

AD, Alzheimer’s disease; Control-i, implanted controls; Control-p, physiological controls; d-AMPH, d-amphetamine; EEG, electroencephalographic; EMG, electromyographic; Hipp,

hippocampus; HVS, high voltage sleep spindle; IBO, ibotenic acid; LDT, laterodorsal tegmental nucleus; MCx, motor cortex; MSN, medium sized spiny neurons; NHS, normal horse serum; NREM, non rapid eye movement; PBS, phosphate buffered saline; PD, Parkinson's disease; PDE, Probability Density Estimate; PPT, pedunculopontine tegmental nucleus; RBD, REM behavioral disorder; REM, rapid eye movement; RT, reticulo-thalamic nucleus; SNpc, substantia nigra pars compacta; TC, thalamo-cortical neurons.

Keywords: sleep, high voltage sleep spindles, Parkinson's disease, pedunculopontine tegmental nucleus, locomotor activity, c-Fos.

1. Introduction

On the base of clinical studies that indicate a heterogeneous cholinergic denervation in PD, with some subjects having maintained and others decreased cortical and/or subcortical activity, it was suggested that PD is a multisystem neurodegeneration, and that differences in the degree or rate of degeneration of different central nervous systems may account for the differences in their phenotypic features [1].

The cortical and thalamic subcortical cholinergic denervations, due to the degeneration of PPT cholinergic neurons, were related to the REM behavioral disorder (RBD) [2], and to gait and balance impairment including falls in PD [3]. The neuropathological studies in humans have reported degeneration of about 50 % of the PPT cholinergic neurons in PD in contrast to

Alzheimer's disease (AD), where no reductions in PPT cholinergic neurons were found [1]. Clinical studies also evidenced the beneficial effect of AChE inhibitor donepezil in 50 % reduction in falls of the PD patients [4]. Therefore, beside the olfactory loss and subtle motor dysfunctions, the RBD presents the prodromal phase of PD [5].

On the other hand, recent studies in the rat model of severely impaired cholinergic thalamo-cortical innervation (the rat model of PD cholinopathy) evidenced the topographically differently expressed EEG microstructures within the sensorimotor and motor cortex during NREM and REM sleep, alongside the appearance of two REM sleep states, particularly within the motor cortex [6,7]. These distinct REM states were differential with regard to: the EEG microstructures, EMG power, and the sensorimotor and motor cortical drives to the dorsal nuchal muscles [8]. In addition, these altered cortical drives were commonly expressed during both REM states as the impaired beta oscillation drive [8], but the sensorimotor cortical drive was altered more severely during "healthy" REM (REM with atonia, theta REM) than during the pathological REM (REM without atonia, sigma REM) sleep.

Moreover, the hallmarks of an earlier aging onset during the impaired thalamo-cortical cholinergic innervation in rat were consistently expressed through the increased EEG sigma amplitude during REM sleep, as a unique REM sleep phenomenon, alongside the broadly altered motor cortical drive to the dorsal nuchal muscles during NREM and REM sleep [9,10].

Generally, the activation state of mammalian neocortex is regulated by a complex interplay of the cortical and subcortical neuronal networks. Whereas the slow EEG oscillations are present in isolated neocortical tissue, the high-frequency oscillations (β and γ frequency oscillations) are not, suggesting a dependence on subcortical impulse flow [11]. The cholinergic afferent fibers system originating in the basal forebrain plays a critical role in switching cortical

activity from deactivated slow to high-frequency activated EEG patterns. Inputs to the cortex, originated in the thalamus, constitute the second major system involved in regulation of cortical activity. The efferent fibers of the PPT (the main thalamo-cortical cholinergic source of innervation) exert, through the thalamus, widespread control over neocortical EEG activation during waking and REM sleep. Because direct projections from the PPT reach both the basal forebrain and thalamus, this nucleus is an ideal candidate to study the integrated contributions of these two cholinergic systems to regulating activation of the neocortex [11].

We have to note here, that the PPT has important functions relevant to the regulation of REM sleep [12,13], arousal [14], and various motor control systems [15], including breathing control [16,17]. It is also postulated that PPT is the high relay nucleus for overall REM sleep phenomenon control, and that each REM sleep event, executed by distinct cell groups within the brainstem, may be triggered and modulated by the activation of the PPT [18].

In addition, the PPT has an important role in hippocampal theta generation [19], but the cellular and network mechanisms accountable for the hippocampal theta oscillations generation are still not fully understood. While the PPT stimulation elicits hippocampal theta accompanied by wakefulness and REM sleep [20], and can induce locomotion, as a part of the mesencephalic locomotor region [21], suppression of the PPT activity abolishes hippocampal theta rhythm in rats [22]. Recent tracing study in rats, that evidenced the PPT as an only extrinsic source of cholinergic innervation of the striatum [23], the brain structure that plays a key role in learning, memory and motor control, opens the new avenues for research of the PPT role in the disorders of motor control during sleep.

All aforementioned clinical and animal studies suggested the sleep disorders, particularly the REM sleep disorders, as the possible functional biomarkers of neurodegeneration that are

relevant to PD, and as the biomarkers of an earlier aging onset in the brain with neurodegeneration vs. physiological (healthy) brain [8,9]. In addition, recent PET imaging studies in humans, which demonstrated the thalamic cholinergic denervation in the PD with or without dementia in contrast to AD, suggested that the neurodegeneration of the thalamic cholinergic afferent projections may contribute to the disease specific motor and cognitive abnormalities [24].

Although the biomarkers of neurodegenerative diseases are critically needed, so far there are no practical, definitive diagnostic or progression biomarkers.

Therefore, in order to find out the possible earliest biomarkers of PD cholinopathy, in this study we followed the impact of bilateral PPT lesion in rat on: the cortical and hippocampal sleep/wake states architectures, all sleep states related EEG microstructures, sleep spindles, on the basal and stimulated locomotor activity, and on the c-Fos immunohistochemical expression in the striatum (caudate putamen), as a biochemical indicator of neuronal activity of the subcortical structure with the most intense dopaminergic input in the brain, and related to the motor control neuronal network.

2. Materials and methods

2.1. Experimental design

We performed the experiments on 29 adult male Wistar rats, 2 and a one half month old at the beginning of the study. We followed sleep and basal locomotor activity throughout the same aging follow-up period (from 14 to 91 days following surgical procedure for the implantation of EEG and EMG electrodes for chronic sleep recording with or without the bilateral PPT lesion). Behavioral assessments were performed during the same circadian phase as

sleep recording (during inactive circadian phase for rats, from 9 a.m. to 3 p.m.), but always a week later to each sleep recording session. We used 22 rats for sleep recording, divided in two groups: the implanted controls (n = 11; Control-i), and the PPT lesioned rats (n = 11; PPT lesion). For the basal behavioral assessments we included additional control group of untreated animals (n = 7; the physiological control – Control-p).

For the behavioral analysis of stimulated locomotor activity, following all sleep and behavioral assessment sessions, after 91 days of surgical procedure, we used the Control-i and PPT lesion group (n = 10 for Control-i; n = 8 for PPT lesion) divided in two subgroups: one for the d-amphetamine injection (d-AMPH; n = 7 for Control-i; n = 5 for PPT lesion), and the other for the saline injection as corresponding sham control (n = 3 for Control-i; n = 3 for PPT lesion).

Prior to surgery and throughout the experimental protocol, the animals were maintained on a 12 h light-dark cycle, and were housed at 25°C with free access to food and water. All experimental procedures were in compliance with EEC Directive (2010/63/EU) on the protection of animals used for experimental and other scientific purposes, and were approved by Ethical Committee for the Use of Laboratory Animals of the Institute for Biological Research “Sinisa Stankovic”, University of Belgrade (Approval N° 2-21/10)

2.2. Surgical procedure

The surgical procedures employed for the EEG and EMG electrodes implantation for chronic sleep recording and the bilateral PPT lesion have been described previously [6-9,25-29] and are outlined below.

We implanted under ketamine/diazepam anesthesia (Zoletil 50, VIRBAC, France, 50 mg/kg; i.p.), in 2 and a one half month old rats, according to Paxinos and Watson [30], two epidural stainless-steel screw electrodes for electroencephalographic (EEG) cortical activity from

the motor cortex (MCx; A/P: +1.0 mm from bregma; R/L: 2.0 mm from sagittal suture; D/V: 1 mm from the skull), two pairs of the stainless-steel teflon-coated wires (Medwire, NY, USA) into the CA1 hippocampal regions (A/P: -3.60 mm from bregma; R/L: 2.5 mm from sagittal suture; D/V: 2.5 mm from the brain surface) as well as into the dorsal nuchal musculature to assess skeletal muscle activity (EMG), and a stainless-steel screw electrode in the nasal bone as a ground. All the electrode leads were soldered to a miniature connector plug (39F1401, Newark Electronics, Schaumburg, IL, USA), and the assembly was fixed to the screw electrodes and skull using acrylic dental cement (Biocryl-RN, Galenika a.d. Beograd, Serbia).

During the surgical procedure for implantation of EEG and EMG electrodes we performed the bilateral PPT lesions. The excitotoxic lesions were induced using the stereotaxically guided microinfusion of 0.1 M IBO/0.1 M phosphate buffered saline (PBS) bilaterally into the PPT (A/P: -7.8 mm from bregma; R/L: 1.9 mm from the sagittal suture; D/V: 7.0 mm from the brain surface), using a Digital Lab Standard Stereotaxic Instrument (Stoelting Co., Europe) with Hamilton syringe (1 μ l). The IBO (Sigma-Aldrich, Germany; pH = 7.4) concentration was chosen on the basis of previous studies [6,8,9,29,31]. The microinfusions were introduced at a volume of 100 nl, using a single, 60 s pulse. Following microinfusion, the Hamilton syringe was left within the local brain tissue for 5 min before removal from the brain, allowing the IBO solution to diffuse within the PPT. After removal from one side of the brain, the needle of Hamilton syringe was always washed out using saline, and then it was positioned again into the PPT of the other brain side, for the next IBO microinfusion.

2.3. Recording procedure

At the end of surgical procedure the scalp wounds were sutured and the rats were allowed to recover for 13 days before their adaptation to the recording cable and plexiglass chamber (30

cm x 30 cm x 30 cm) for one day. The EEG and EMG activities were carried from the connector plug on the rat head by cable, passed through a sealed port on the recording box, and differentially recorded. The differential mode consisted of 6 inputs (left MCx, right MCx, left Hipp, right Hipp, left EMG, right EMG), each with a (+) on the left and a (-) on the right side, and all with the same ground (a screw electrode implanted in the nasal bone). The EEG and EMG activities were displayed on a computer monitor, and stored on disk for further off-line analysis. After conventional amplification and filtering (0.3 – 100 Hz band pass; A-M System Inc. Model 3600, Calborg, WA, USA), the analog data were digitized (at the sampling frequency of 256/s) and recorded for 6 h, during the normal inactive circadian phase for rats (from 9 a.m. to 3 p.m.) using DataWave SciWorks Experimenter Version 8.0 (DataWave Technologies, Longmont, CO, USA). In this study the sleep recording sessions of spontaneous sleep were done in all rats (Control-i and PPT lesion) 14, 42, and 91 days after surgical procedure and/or the PPT lesion.

2.4. Behavioral assessments

Following a week of each sleep recording session, the basal locomotor activity has been tested, during the same circadian phase as for the sleep recording sessions (from 9 a.m. to 3 p.m.). The behavioral tests were done following 30 min of habituation to the experimental room, over 30 min, by the open-field test using the Opto-Varimex Auto-Track System (Columbus Instruments, OH, USA). For the assessment of basal locomotor activity we used 7 rats per each experimental group (n = 7; Control-p, Control-i, PPT lesion).

At the end of all sleep recording and basal locomotor activity sessions (up to 91 days after surgical procedure and/or the PPT lesion) the locomotor activity of Control-i (n = 7), and PPT lesion group (n = 5) was additionally examined after the stimulation with d-AMPH (1.5

mg/kg dissolved in saline, in a final volume 0.5 ml/kg, i.p.) or after the saline injection (0.5 ml/kg saline, i.p.; n = 3 per each group), which served as the corresponding sham controls. Locomotor activity was monitored immediately after the treatment, for the next 2 h [32]. Following the post-amphetamine or post-saline behavioral assessments we immediately and deeply anesthetized all rats (Zoletil 50, VIRBAC, France, 100 mg/kg; i.p.), for their transcardial perfusion.

2.5. Tissue processing for histochemistry and immunohistochemistry

We identified the PPT and caudate putamen lesions by NADPH - diaphorase histochemistry [33]. The rats were deeply anesthetized and perfused transcardially, starting with a vascular rinse until the liver had been cleared (200 ml of 0.9 % saline; perfusion speed of 40 ml/min); followed by a 4 % paraformaldehyde solution in 0.1 M PBS (200 ml; 100 ml at 40 ml/min, and then 30 ml/min), and finally with the 10 % sucrose solution in 0.1 M PBS (200 ml; 30 ml/min). The animals were sacrificed and the brains were extracted, cleared of the meninges and blood vessels, and immersed in 4 % paraformaldehyde overnight, and then in 30 % sucrose solution for several days. The brains were cut in a coronal plane into 40 μ m-thick sections using a cryotome, and the free-floating sections were stained, mounted, and cover slipped with DPX (Sigma), and then examined under a Zeiss Axiovert microscope equipped with a camera. Briefly, the free-floating sections were rinsed in 0.1 M PBS, pH = 7.4, and incubated for 1 h at 37°C in the staining solution – a mixture of the substrate solution with β -nicotinamide adenine dinucleotide phosphate, reduced Na₄ salt (β -NADPH, Serva, Heidelberg, Germany), and dimethyl sulfoxide (DMSO, Sigma). The substrate solution contained dissolved nitro blue tetrazolium chloride (NBT, Serva), and 5bromo-4chloro-3indolyl phosphate (BCIP, Serva) in the substrate buffer with pH = 9.5 (0.1 M Tris, 100 mM NaCl, 5 mM MgCl₂). To reduce the

background staining coming from endogenous alkaline phosphate, the specific inhibitor levamisole (Sigma) was added to the staining solution to produce the final concentration of 2 mM [6,9,27].

All the tissue samples, of all the experimental groups, and per each brain structure were grouped into three defined stereotaxic ranges of the PPT and the caudate putamen rostro-caudal dimensions. We quantified the cholinergic cell loss using Image J 1.46 software. NADPH - diaphorase positive cells were counted in three 40 μ m thick coronal sections for each brain within the overall rostro-caudal dimension of each structure. The number of NADPH - diaphorase positively stained cells was intended to provide an estimate of the lesion damage or the cholinergic neuronal numbers, rather than an attempt to determine the absolute numbers of cholinergic neurons. The cholinergic neuronal loss was expressed for each brain side and for each defined stereotaxic range within the overall rostro-caudal dimension of each brain structure, as the percent difference of NADPH - diaphorase positive cells versus the controls. To be specific, all the percentage differences were expressed with respect to the mean control absolute numbers for each stereotaxic range of each brain structure, which was taken as 100 % [6,9,27].

In addition we did the c-Fos immunohistochemistry in the caudate putamen to follow the changes in neuronal activity following the amphetamine test, caused by the bilateral PPT lesion. Immunohistochemistry was performed under the same conditions for all experimental samples using avidin–biotin complex (ABC) method (VECTASTAIN Universal Elite ABC-Peroxidase Kit, Vector Laboratories, Burlingame, CA, USA). Brain sections were initially thoroughly rinsed with 0.1 M PBS (pH = 7.4). The endogenous peroxidase activity was neutralized with 3 % hydrogen peroxide/10 % methanol for 15 min, and the nonspecific binding was prevented by 30 min incubation in normal horse serum (NHS)/0.1 M PBS at room temperature. The sections were

further incubated overnight at 4°C with rabbit anti-c-Fos antibody (sc-52, Santa Cruz, Dallas, Texas, USA) diluted in 1 % NHS/0.1 M PBS. Biotinylated horse anti-mouse/rabbit IgGs was subsequently used (for 1 h), followed by 30 min incubation with VECTASTAIN ABC reagent/0.1 M PBS. Between each immunolabeling step, sections were washed in fresh 0.1 M PBS (3 x 5 min). Immunoreactive signals were visualized using 3,3'-diaminobenzidine as a chromogen (DAB Peroxidase Substrate Kit, Vector Laboratories). Finally, all sections were mounted on the slides, dehydrated in a series of increasing ethanol solutions (Ethanol 70 %, 96 %, 100 %, Zorka Pharma, Serbia), cleared (Xylene, Zorka Pharma, Serbia), mounted with DPX (Sigma), and cover-slipped. To test immunolabeling specificity, the primary antibodies were omitted in control experiments.

2.6. Data Analysis

The analysis of the sleep recorded signals was conducted using software developed in MATLAB 6.5 [6-9,29], and upgraded to MATLAB R2011a. We applied Fourier analysis to signals acquired throughout 6 h (2160 10 s Fourier epochs), and each 10 s epoch was differentiated, on the base of EEG and EMG, as the Wake, NREM or REM state. The differentiation of all Wake/NREM/REM epochs was improved by using the logarithmic values of the quantities on both EEG and EMG axes, and was finally achieved using the two clusters K means algorithm [6-9,27-29].

In this study, we particularly extracted the simultaneous Wake/NREM/REM 10 s epochs of the motor cortex (MCx) and hippocampus (Hipp) for sleep architecture analysis as well as for all state-related EEG microstructures analysis from each brain structure (the relative amplitudes of all the conventional EEG frequency bands during Wake/NREM/REM) by using the

Probability Density Estimate (PDE) routine supplied with MATLAB R2011a [6,8,9,29]. The typical examples of the scatter-grams of simultaneous (common) sleep/wake states, differentiated and extracted from the MCx and Hipp, are depicted in **Fig. 1**.

In addition, for each sleep/wake state and each frequency band, PDE analysis was performed on the assembles of relative amplitudes by pooling measured values from all animals belonging to specific experimental (Control-i or PPT lesion) and age group (14, 42, 91 days after the surgical procedure for implantation of EEG and EMG electrodes for chronic sleep recording with or without the bilateral PPT lesion).

In order to identify the high voltage sleep spindles (HVS) we combined automatic detection with visual validation of all detected HVS for their final visual extraction. Namely, the first step for automatic HVS detection during REM sleep was to concatenate all the extracted 10 s epochs of simultaneous REM sleep from the MCx and Hipp of each rat, each experimental group, each age group, and to filter the EEG signals using the 4.1 – 10 Hz band pass filter. Then, we applied the Continuous Wavelet Transform with the mother wavelet “cmor1-2“ MATLAB R2011a function, providing a complex Morlet wavelet with determined central frequency $f_0 = 2$ [34]. In addition, all HVS had a minimal duration of 0.5 s.

Since we automatically detected many false positive HVS, we visually corrected the automatically detected HVS, and visually extracted them for each simultaneous REM sleep episode of each brain structure, each rat, each experimental group, and throughout the overall aging follow-up period, and then we concatenated them for the analysis of HVS dynamics (density, duration, and frequency per 6 h of sleep).

For the statistical analyses of the basal locomotor activity we calculated the means for 5 min periods for the time-line profiles, and the means \pm SE for totals of 30 min periods.

Changes in locomotor activity following stimulation by d-AMPH injection were presented as the means per 10 min and the means \pm SE per 120 min intervals.

All statistical analyses were done using Kruskal-Wallis ANOVA with the Mann Whitney U two-tailed post-hoc test. The accepted level of significance was $p \leq 0.05$.

3. Results

3.1. Histological identification of the PPT lesion and its remote impact within the caudate putamen

We have evidenced the mean PPT cholinergic neuronal loss $> 22\%$ throughout the overall PPT dimension on each brain side, with the maximal loss of $30.68 \pm 6.28\%$ caudally (**Fig. 2**). In addition, the mean remote cholinergic neuronal loss within the caudate putamen was also $> 26\%$ throughout the overall putamen dimension on each brain side, with the maximal loss of $31.18 \pm 14.13\%$ also caudally (**Fig. 3**).

Since we have used for the quantification three .tiff images of the $40\ \mu\text{m}$ sections per each brain structure of each rat, the manually counted numbers of NADPH - diaphorase positively stained cells, using the Image J 1.46, provided an estimate rather than the absolute numbers of cholinergic neurons within the overall rostro-caudal dimension of PPT or the caudate putamen.

3.2. Alteration of locomotor activity following the PPT lesion

Basal locomotor activities during all examined time points after the surgery are presented in **Fig. 4**. During the first test session there was no statistical differences in locomotor activity between the Control-p, Control-i and the PPT lesion rats (Day 14; $X^2 = 0.99$, $p = 0.61$). However, there was the significant decrease of locomotor activity during the second test session

(Day 42; $X^2 = 8.97$, $p = 0.01$), due to the PPT lesion (* $z = -2.36$, $p = 0.02$, vs. Control-p; # $z = -2.75$, $p = 0.01$, vs. Control-i), which lasted up to 91 days after the surgical procedure (Day 91; $X^2 = 7.52$, $p = 0.02$; * $z = -1.98$, $p = 0.04$, vs. Control-p; # $z = -2.69$, $p = 0.01$, vs. Control-i). There were no significant differences between the locomotor activity of Control-p and Control-i group neither during the second (Day 42; $z = -0.19$, $p = 0.85$) nor during the third testing session (Day 91; $z = -0.83$, $p = 0.41$).

3.3. Sleep architecture, sleep/wake state related EEG microstructure, and HVS dynamics following the PPT lesion

The bilateral PPT lesion did not change sleep/wake states architecture within the MCx and Hipp during the overall follow-up period ($z \geq -2.01$, $p \geq 0.14$; data not shown), but there was the severe and long-term EEG microstructure disorder during NREM sleep, expressed earlier than the decreased locomotor activity only within the Hipp, from 14 to 42 days (**Fig. 5**), and simultaneously in the Hipp and MCx 91 days after the PPT lesion (**Fig. 6**). Apart from the onset of NREM sleep disorder, that was earlier and longer within the hippocampus (**Fig. 5**; **Fig. 6**), it was mainly expressed as the augmented delta amplitude and attenuated beta amplitude both at the hippocampal ($z \geq -3.55$, $p \leq 0.003$) and motor cortical ($z \geq -2.61$, $p \leq 0.04$) level.

When we visually detected within the analog EEG signals, recorded from the MCx and Hipp, the occurrence of the HVS during their simultaneous REM sleep, visually determined as the 9 Hz oscillations, we additionally filtered these signals in the expanded theta range (4.1 – 10 Hz) to particularly follow the changes of its relative amplitude due to the occurrence of the HVS. This approach enables us to detect the simultaneously augmented expanded theta amplitude due to more frequent occurrence of the HVS during REM (**Fig. 7**) in the MCx and Hipp 42 days after the PPT lesion ($z \geq -2.86$, $p \leq 0.05$), that lasted 91 days after the PPT lesion only in the MCx ($z =$

2.98, $p = 0.003$). But, following visual extraction of the HVS during simultaneous REM sleep of the MCx and Hipp of each rat, that were concatenated per each brain structure, each experimental group (Control-i and the PPT lesion), and throughout the overall aging follow-up period (from 14 to 91 days after surgical procedure), we were able to evidence more specifically that: the PPT lesion permanently increased the HVS density during REM sleep within both brain structures (**Table 1**; $z \geq -2.59$, $p \leq 0.05$) from 14 to 91 days after the PPT lesion, and significantly decreased HVS intrinsic frequency only within the Hipp ($z = -4.91$, $p = 10^{-4}$; **Table 1**; **Fig. 8B** right panels; left shifted black distribution). Moreover, whereas the PPT lesion permanently prolonged the HVS within the MCx ($z = -4.56$, $p = 10^{-4}$; **Table 1**; **Fig. 8A** left panels; right shifted black distribution), it shortened the HVS within the Hipp ($z = -4.37$, $p = 10^{-4}$; **Table 1**; **Fig. 8B** left panels; left shifted black distribution) during their simultaneous REM sleep. In addition, there was a stable inter-structure difference of the mean HVS duration and intrinsic frequency which were always shorter and slower in the Hipp vs. the MCx (**Table 1**).

Fig. 8 depicts also the individual examples of 30 s analog signals with the HVS during simultaneous REM sleep of the MCx and Hipp in the Control-i and PPT lesioned rat, that represent the group data (**Fig. 8A,B** three upper panels).

For the group probability density distributions of the HVS durations and intrinsic frequency depicted in **Fig. 8A,B**, we included the assembles of 414 HVS for the MCx, and 248 HVS for the Hipp of the Control-i rats; and the assembles of 1338 HVS for the MCx, and 1449 HVS for the Hipp of the PPT lesioned rats.

3.4. Effect of the amphetamine on locomotor activity and neuronal activity within the caudate putamen

We have shown the long-lasting decrease of locomotor activity or “hypokinesia” (**Fig. 4**) with an onset from 42 days after the bilateral PPT lesion. Paradoxically, in these “hypokinetic” rats (PPT lesion group) d-AMPH injection induced the significantly higher increment of locomotor activity (“hyperactivity”) vs. the Control-i rats (**Fig. 9A**, $*z = -2.03$, $p = 0.04$). On the other hand there was no difference in the locomotor activity between the Control-i sham controls and the PPT lesion sham controls (data not shown, $z = -0.22$, $p = 0.83$)

Moreover, the augmented locomotor activity in the PPT lesioned rats, caused by d-AMPH stimulation (**Fig. 9A**), was underlined by the suppressed c-Fos immunoreactivity in the caudate putamen (**Fig. 9B**, bottom panels) with respect to Control-i rats (**Fig. 9B**, upper panels).

Fig. 9B depicts the individual examples of suppressed c-Fos immunoreactivity by d-AMPH injection in the caudate putamen of three PPT lesioned rats (**Fig. 9B**, bottom panels) vs. three Control-i rats (**Fig. 9B**, upper panels).

4. Discussion

We demonstrated for the first time, that the earliest and long-lasting biomarker of the PD cholinopathy in rat was the NREM sleep disorder in the Hipp (**Fig. 5**), alongside the altered HVS dynamic (**Table 1**; **Fig. 8**) in both the Hipp and MCx during their simultaneous REM sleep. This altered and long-lasting EEG microstructure of the Hipp during NREM sleep was mainly expressed as the augmented delta amplitude and attenuated beta amplitude, and became common in the Hipp and MCx during NREM 91 days after the PPT lesion (**Fig. 6**). Apart from the slowness of NREM sleep, the bilateral PPT lesion increased HVS density in both brain structures, during their common REM sleep (**Table 1**), prolonged HVS duration in the motor cortex (**Fig. 8A**), but decreased the HVS duration and frequency in the hippocampus (**Fig. 8B**). Namely, the slower NREM sleep of the Hipp was followed by the slower HVS during REM

sleep. In addition, there was the long-lasting decrease of locomotor activity (“hypokinesia”) developed 42 days following the bilateral PPT lesion (**Fig. 4**). Moreover, we have shown that during this delayed and long-lasting “hypokinesia”, caused by the PPT lesion, d-amphetamine stimulation augmented locomotor activity much more than in the controls (**Fig. 9A**) with an underlying suppression of neuronal activity in the caudate putamen (**Fig. 9B**).

Sleep disorders such as the restless leg syndrome, RBD, sleep fragmentation, insomnia, excessive daytime sleepiness precede the motor impairments in PD patients [35], and the brain structures associated with sleep regulation (such as the locus coeruleus, lower raphe nuclei and PPT) are affected before the substantia nigra pars compacta (SNpc) [36]. On the other hand, there is evidence for a role of dopaminergic neurotransmission in regulating some aspects across the sleep/wake cycle [37], as well as the lesion of SNpc or blockade of D2 receptors reduced a time spent in REM sleep [38,39].

Anatomically, the basal ganglia and the PPT share many similarities. They are both the heterogeneous structures that have similar patterns of inputs and outputs, including cortex, thalamus, amygdala and brainstem [40]. In addition to its ascending projections to the thalamus, the PPT is also connected with basal ganglia, cerebral cortex, and the brainstem reticulospinal tract [41]. Among these connections the PPT has a unique reciprocity with the basal ganglia [40]. Electrical stimulation of the PPT induces a burst firing of dopaminergic neurons [42], release of dopamine in the striatum [43], and induces locomotion [44].

In addition, the basal ganglia and the PPT share similar functions concerning locomotion, memory consolidation and sleep regulation [40]. Furthermore, recent study provided the novel evidence for the association of the PPT and basal ganglia in NREM and REM sleep regulation, and suggested a new circuitry for sleep regulation in the PD – the triad composed of PPT, SNpc

and striatum [45]. Also, on the base of recent evidence for the functional connectivity of the PPT and deep cerebellar nuclei [46], it was suggested that the PPT, beside its important role in the cortico-basal ganglia circuit, may act as an interface device between the basal ganglia and cerebellum, thereby influencing motor control and cognitive functions [41].

PPT is the major source of acetylcholine for the SNpc, and the cholinergic efflux from the PPT to SNpc is an important source of nigrostriatal pathway activation or excitation [47,48]. Recent study evidenced that the PPT and laterodorsal tegmental nucleus (LDT) constitute the only external source of cholinergic innervation of the striatal complex [23], and while the PPT predominantly targets the dorsolateral striatum, the LDT targets the dorsomedial striatum and nucleus accumbens [48].

In our study we evidenced the PPT cholinergic neuronal loss $> 22\%$ throughout the overall PPT dimension on each brain side, with the maximal loss of $30.68 \pm 6.28\%$ caudally that induced the remote cholinergic neuronal loss within the caudate putamen $> 26\%$ throughout the overall putamen dimension on each brain side, with the maximal loss of $31.18 \pm 14.13\%$, also caudally. In our previous studies [6,7,9,27,29], as in this study, we bilaterally lesioned the PPT pars compacta as the 90% cholinergic part of the PPT, and we induced, using the same methodological approach as in this study, the same and persistent cholinergic neuronal loss in the PPT with no progression from 14 to 91 days following the bilateral PPT lesion [9]. In addition, in this study we identified the cholinergic neuronal loss in the PPT and its remote effect in the caudate putamen only 91 days after the bilateral PPT lesion, after all sleep recording and behavioral test sessions, not across the overall follow-up period, so we do not have an evidence for the onset of the remote cholinergic neuronal loss in the caudate putamen.

Our present results have shown that following the onset of NREM sleep disorder in the Hipp, along with altered HVS dynamics during REM sleep in both the Hipp and MCx, there was a delayed decrease of locomotor activity (“hypokinesia”) expressed from 42 to 91 days after the PPT lesion, probably due to a tonically decreased excitation of the nigrostriatal dopaminergic pathway. Furthermore, when we stimulated the locomotor activity by d-amphetamine injection, these “hypokinetic” rats responded with the locomotor hyperactivity. After this locomotor hyperactivity in the PPT lesioned rats we evidenced a suppression of neuronal activity in the caudate putamen, suggesting the further shift of an imbalance between the direct and indirect pathway of the basal ganglia motor circuits, i.e. the inhibition of indirect pathway that contributes to the relief of direct pathway activity leading to the more prominent locomotor activity than in controls.

It is important to note here, that although the caudate putamen is heterogeneous structure, these suppressed neurons in our present study are probably GABA projection neurons (medium sized spiny neurons; MSN) since they present 90 % of neurons in the caudate putamen, beside 10 % of interneurons, respectively [49]. On the other hand, the largest group of interneurons within the caudate putamen is the cholinergic aspiny neurons, or so called tonically active interneurons, along with three types of GABA interneurons (the parvalbumin, calretinin and nitrenergic GABA interneurons). The cholinergic interneurons are the giant cells that represent about 1 % of the total population of striatal neurons, but send widely projections throughout the striatum, establishing the synaptic contacts. It appears that dopamine inhibit the striatal cholinergic interneurons, which are therefore overactive in the PD and in turn inhibit dopamine release by muscarinic receptors, creating a vicious cycle [50].

In addition, the striatum contains the glutamatergic afferents from the cerebral cortex, thalamus, amygdala; serotonergic afferents from the dorsal raphe nucleus; as well as the dopaminergic afferents arising from the SNpc [49,], and the cholinergic afferents arising from the PPT [23]. It is important to note here, that the nigrostriatal axons synapse with MSN and excite or inhibit them depending on their D1 or D2 containing receptors (dopaminergic afferents excite D1 MSN, but inhibit D2 MSN).

In our present study there was a tonically impaired cholinergic afferent innervation of the caudate putamen and SNpc, from the PPT, and tonically decreased number of the striatal cholinergic interneurons. In this condition the phasic activation of the dopaminergic neurons by amphetamine were expressed as “hyperkinesia”, probably due to re-organizational hypersensitivity of MSN neurons to dopamine inhibition (probably the hypersensitivity of D2 receptors).

Regarding the alteration of HVS dynamics, demonstrated during common REM sleep in both brain structures in our study, we have to mention that sleep spindles present the basic thalamo-cortical EEG rhythms typically expressed during light NREM sleep, or during transition from NREM to REM sleep. Sleep spindles, reflecting the bursting mode of thalamo-cortical neuronal activity, arise the awakening threshold. Their role has been debated for a long time, but it is now believed that they contribute in sleep promotion and maintenance associated to sensory gating, cognition and memory consolidation. There is also an evidence for the increased functional connectivity between hippocampus and cortex during the appearance of sleep spindles [51]. In addition, sleep spindles, defined as the biomarkers of brain function and plasticity, present a neural correlate of the loss of consciousness, prevent stimuli to reach consciousness or prevent an integration of brain activity, and have an important role in sleep-dependent memory

improvement [52]. Also, the underlying neurochemical background of REM sleep (an increase of acetylcholine and a decrease of monoamines during REM sleep) facilitate protein synthesis and long-term potentiation in the hippocampus [53]. Moreover, altered sleep spindle dynamics have been documented in coma, epilepsy, dyslexia, schizophrenia, stroke, and many other forms of mental diseases [54].

In addition, there is increasing evidence in human [55] and animal studies [56] that abnormally synchronized oscillatory activity in the cortico-basal ganglia loop is associated with the motor deficits in PD, particularly beta synchronization (14 – 30 Hz) and HVS (5 – 13 Hz). Our present results in the rat model of PD cholinopathy are in accordance with evidence that dopamine depletion in 6-OHDA lesioned rats increase the density and duration of HVS, as a particular pattern of spindle activity that also reflects the state of thalamo-cortical regulatory network during PD [55].

Spindle frequency is basically determined by the interplay of GABAergic inhibitory neurons of the reticulo-thalamic (RT) nucleus and the thalamo-cortical (TC) neurons, their intrinsic properties, and their influence by cortical descending and the brainstem ascending inputs. The duration of IPSPs imposed by RT neurons on TC neurons determines the intra-spindle frequency [52].

Since the PPT cholinergic afferents inhibit RT neurons, the increased density of prolonged HVS in the MCx vs. the increased density of slower and shorter HVS in the Hipp during REM sleep, in our present study, reflects serious changes within the thalamo-cortical regulatory network during REM sleep. These re-arrangements within the thalamo-cortical regulatory network might be due to the tonically and sustainably decreased cholinergic inhibition of RT neurons and excitation of TC neurons across all sleep/wake states, particularly during

REM sleep, as well as a tonically decreased excitation of the nigrostriatal dopaminergic afferents to the striatum with decreased number of the cholinergic interneurons in the basal ganglia-thalamo-cortical regulatory network.

Impact of a tonically impaired PPT cholinergic innervation in our study was expressed earlier as sleep disorder then as movement disorder. This sleep disorder was the earliest, and long-lasting at hippocampal and thalamo-cortical level, followed by a delayed “hypokinesia”. In our rat model of PD cholinopathy there was a serious impact of a tonically impaired PPT cholinergic innervation on cholinergic interneurons of the caudate putamen, as well as on its regulatory network in motor control.

Our study indicate that in order how they occurred, the hippocampal NREM sleep disorder, altered HVS dynamics during REM sleep in the hippocampus and motor cortex, and „hypokinesia” may serve as the biomarkers of PD cholinopathy onset and progression.

Conflict of interest

The authors declare no conflict of interest

Acknowledgement: This work was supported by Serbian Ministry of Education, Science and Technological Development Grants OI 173022 and OI 173056.

References

- [1] N.I. Bohnen, R.L. Albin, The cholinergic system and Parkinson disease, *Behav. Brain Res.* 221 (2011) 564-573. doi: [10.1016/j.bbr.2009.12.048](https://doi.org/10.1016/j.bbr.2009.12.048).
- [2] V. Kotagal, R.L. Albin, M.L. Müller, R.A. Koeppe, R.D. Chervin, K.A. Frey, N.I. Bohnen, Symptoms of rapid eye movement sleep behavior disorder are associated with cholinergic denervation in Parkinson disease, *Ann. Neurol.* 71 (2012a) 560-568. doi: [10.1002/ana.22691](https://doi.org/10.1002/ana.22691).

- [3] N.I. Bohnen, M.I. Müller, R.A. Koeppe, S.A. Studenski, M.A. Kilbourn, K.A. Fey, R.L. Albin, History of falls in Parkinson disease is associated with reduced cholinergic activity, *Neurology* 73 (2009) 1670-1676. doi: [10.1212/WNL.0b013e3181c1ded6](https://doi.org/10.1212/WNL.0b013e3181c1ded6).
- [4] K.A. Chung, B.M. Lobb, J.G. Nutt, F. Horak, Cholinergic augmentation in frequently falling subjects with Parkinson's disease, *Mov. Disord.* 24 (Suppl 1) (2009) S259. doi: [10.1002/mds.22628/epdf](https://doi.org/10.1002/mds.22628/epdf).
- [5] S. Przedborski, The two-century journey on Parkinson disease research, *Nature Neurosci.* 18 (2017) 251-259. doi: [10.1038/nrn.2017.25](https://doi.org/10.1038/nrn.2017.25).
- [6] J. Petrovic, J. Ciric, K. Lazic, A. Kalauzi, J. Saponjic, Lesion of the pedunclopontine tegmental nucleus in rat augments cortical activation and disturbs sleep/wake state transitions structure. *Exp. Neurol.* 247 (2013a) 562-571. doi: [10.1016/j.expneurol.2013.02.007](https://doi.org/10.1016/j.expneurol.2013.02.007).
- [7] J. Petrovic, K. Lazic, J. Ciric, A. Kalauzi, J. Saponjic, Topography of the sleep/wake states related EEG microstructure and transitions structure differentiates the functionally distinct cholinergic innervation disorders in rat, *Behav. Brain Res.* 256 (2013b) 108-118. doi: [10.1016/j.bbr.2013.07.047](https://doi.org/10.1016/j.bbr.2013.07.047).
- [8] J. Petrovic, K. Lazic, A. Kalauzi, J. Saponjic, REM sleep diversity following the pedunclopontine tegmental nucleus lesion in rat, *Behav. Brain Res.* 271 (2014) 258-268. doi: [10.1016/j.bbr.2014.06.026](https://doi.org/10.1016/j.bbr.2014.06.026).

- [9] J. Ciric, K. Lazic, J. Petrovic, A. Kalauzi, J. Saponjic, Age-related disorders of sleep and motor control in the rat models of functionally distinct cholinergic neuropathology, *Behav. Brain Res.* 301 (2016) 273-286. doi: [10.1016/j.bbr.2015.12.046](https://doi.org/10.1016/j.bbr.2015.12.046).
- [10] J. Ciric, K. Lazic, J. Petrovic, A. Kalauzi, J. Saponjic, Sleep spindles as an early biomarker of REM sleep disorder in a rat model of Parkinson's disease cholinopathy, *Transl. Brain Rhythmicity* 2(1) (2017) 1-11. doi: [10.15761/TBR.1000111](https://doi.org/10.15761/TBR.1000111).
- [11] H.C. Dringenberg, M.C. Olmstead, Integrated contributions of basal forebrain and thalamus to neocortical activation elicited by pedunculopontine tegmental stimulation in urethane-anesthetized rats, *Neuroscience* 119 (2003) 839-853. doi: [10.1016/S0306-4522\(03\)00197-0](https://doi.org/10.1016/S0306-4522(03)00197-0).
- [12] R.W. McCarley, J.A. Hobson, Neuronal excitability modulation over the sleep cycle: a structural and mathematical model, *Science* 189 (1975) 58-60. doi: [10.1126/science.1135627](https://doi.org/10.1126/science.1135627).
- [13] J. Lu, D. Sherman, M. Devor, C.B. Saper, A putative flip-flop switch for control of REM sleep, *Nature* 441 (2006) 589-594. doi: [10.1038/nature04767](https://doi.org/10.1038/nature04767).
- [14] S. Datta, R.R. MacLean, Neurobiological mechanisms for the regulation of mammalian sleep-wake behavior: reinterpretation of historical evidence and inclusion of contemporary cellular and molecular evidence, *Neurosci. Biobehav. Rev.* 31 (2007) 775-824. doi: [10.1016/j.neubiorev.2007.02.004](https://doi.org/10.1016/j.neubiorev.2007.02.004).

- [15] K. Takakusaki, T. Habaguchi, K. Saitoh, J. Kohyama, Changes in the excitability of hindlimb motoneurons during muscular atonia induced by stimulating the pedunculopontine tegmental nucleus in cats, *Neuroscience* 124 (2004) 467-480. doi: [10.1016/j.neuroscience.2003.12.016](https://doi.org/10.1016/j.neuroscience.2003.12.016).
- [16] J. Saponjic, M. Radulovacki, D.W. Carley, Respiratory pattern modulation by the pedunculopontine tegmental nucleus, *Respir. Physiol. Neurobiol.* 138 (2003) 223-237. doi: [10.1016/j.resp.2003.08.002](https://doi.org/10.1016/j.resp.2003.08.002).
- [17] J. Saponjic, J. Cvorovic, M. Radulovacki, D.W. Carley, Serotonin and noradrenaline modulate respiratory pattern disturbances evoked by glutamate injection into pedunculopontine tegmentum of anesthetized rats, *Sleep* 28 (2005) 560-570. doi: [10.1093/sleep/28.5.560](https://doi.org/10.1093/sleep/28.5.560).
- [18] S. Datta, Cellular basis of pontine ponto-geniculo-occipital wave generation and modulation, *Cell. Mol. Neurobiol.* 17 (1997) 341-365. doi: [10.1023/A:1026398402985](https://doi.org/10.1023/A:1026398402985).
- [19] M. Pignatelli, A. Beyeler, X. Leinekugel, Neural circuits underlying generation of theta oscillations, *J. Physiol. Paris* 106 (2012) 81-92. doi: [10.1016/j.jphysparis.2011.09.007](https://doi.org/10.1016/j.jphysparis.2011.09.007).
- [20] S. Datta, D.F. Siwek, Excitation of the brain stem pedunculopontine tegmentum cholinergic cells induces wakefulness and REM sleep, *J. Neurophysiol.* 77 (1997) 2975-2988.
- [21] R.D. Skinner, E. Garcia-Rill, The mesencephalic locomotor region (MLR) in the rat, *Brain Res.* 323 (1984) 385-389. doi: [0.1016/0006-8993\(84\)90319-6](https://doi.org/10.1016/0006-8993(84)90319-6).

- [22] A. Nowacka, E. Jurkowlanec, W. Trojnar, Microinjection of procaine into the pedunculopontine tegmental nucleus suppresses hippocampal theta rhythm in urethane-anesthetized rats, *Brain Res. Bull.* 58 (2002) 377-384. doi: [10.1016/S0361-9230\(02\)00801-8](https://doi.org/10.1016/S0361-9230(02)00801-8).
- [23] D. Dautan, H.H. Bay, J.P. Bolam, T.V. Gerdjikov, J. Mena-Segovia, Extrinsic sources of cholinergic innervation of the striatal complex: a whole-brain mapping analysis, *Front. Neuroanat.* 10 (2016) 1-10. doi: [10.3389/fnana.2016.00001](https://doi.org/10.3389/fnana.2016.00001).
- [24] V. Kotagal, M.L. Müller, D.I. Kaufer, R.A. Koeppe, N.I. Bohnen, Thalamic cholinergic innervation is spared in Alzheimer disease compared to parkinsonian disorders, *Neurosci. Lett.* 514 (2012b) 169-172. doi: [10.1016/j.neulet.2012.02.083](https://doi.org/10.1016/j.neulet.2012.02.083).
- [25] J. Saponjic, M. Radulovacki, D.W. Carley, Monoaminergic system lesions increase post-sigh respiratory pattern disturbance during sleep in rats, *Physiol. Behav.* 90 (2007) 1-10. doi: [10.1016/j.physbeh.2006.08.019](https://doi.org/10.1016/j.physbeh.2006.08.019).
- [26] J. Ciric, K. Lazic, J. Petrovic, A. Kalauzi, J. Saponjic, Aging induced cortical drive alterations during sleep in rats, *Mech. Ageing Dev.* 146-148 (2015) 12-22. doi: [10.1016/j.mad.2015.03.002](https://doi.org/10.1016/j.mad.2015.03.002).
- [27] K. Lazic, J. Petrovic, J. Ciric, A. Kalauzi, J. Saponjic, Impact of anesthetic regimen on the respiratory pattern, EEG microstructure and sleep in the rat model of cholinergic Parkinson's

disease neuropathology, Neuroscience 304 (2015) 1-13. doi:
[10.1016/j.neuroscience.2015.07.020](https://doi.org/10.1016/j.neuroscience.2015.07.020).

[28] J. Saponjic, J. Petrovic, J. Ciric, K. Lazic, Disorders of sleep and motor control during the impaired cholinergic innervation in rat – relevance to Parkinson’s disease, in: J. Dorszewska, W. Kozubski (Eds.), Challenges in Parkinson’s Disease, InTech, Rijeka, Croatia, Ch. 7, 2016, pp. 135-153. doi: [10.5772/62949](https://doi.org/10.5772/62949).

[29] K. Lazic, J. Petrovic, J. Ciric, A. Kalauzi, J. Saponjic, REM sleep disorder following general anesthesia in rats, Physiol. Behav. 168 (2017) 41-54. doi:
[10.1016/j.physbeh.2016.10.013](https://doi.org/10.1016/j.physbeh.2016.10.013).

[30] G. Paxinos, C. Watson, The Rat Brain in Stereotaxic Coordinates, fifth ed., Elsevier Academic Press, San Diego, USA, 2005. ISBN: 9780080474120.

[31] W.L. Inglis, K. Semba, Discriminable excitotoxic effects of ibotenic acid, AMPA, NMDA and quinolinic acid in the rat laterodorsal tegmental nucleus, Brain Res. 755 (1997) 17-27. doi:
[10.1016/S0006-8993\(97\)00101-7](https://doi.org/10.1016/S0006-8993(97)00101-7).

[32] V. Pesic, D. Milanovic, J. Popic, K. Smiljanic, V. Tesic, S. Kanazir, V. Jevtovic-Todorovic, S. Ruzdijic, Neonatal propofol anesthesia modifies activity-dependent processes and induces transient hyperlocomotor response to d-amphetamine during adolescence in rats, Int. J. Dev. Neurosci. 47 (2015) 266-277. doi: [10.1016/j.ijdevneu.2015.09.009](https://doi.org/10.1016/j.ijdevneu.2015.09.009).

- [33] G. Paxinos, C. Watson, P. Carrive, M. Kirkcaldie, K.W.S. Ashwell, Chemoarchitectonic Atlas of The Rat Brain, second ed., Academic Press, London, UK, 2009. ISBN: 0123742374.
- [34] M. Adamczyk, L. Genzel, M. Dresler, A. Steiger, E. Friess, Automatic Sleep Spindle Detection and Genetic Influence Estimation Using Continuous Wavelet Transform, *Front. Hum. Neurosci.* 9 (2015) 1-20. doi: [10.3389/fnhum.2015.00624](https://doi.org/10.3389/fnhum.2015.00624).
- [35] M.M. Lima, Sleep disturbances in Parkinson's disease: the contribution of dopamine in REM sleep regulation, *Sleep Med. Rev.* 17 (2013) 367-375. doi: [10.1016/j.smrv.2012.10.006](https://doi.org/10.1016/j.smrv.2012.10.006).
- [36] H. Braak, E. Ghebremedhin, U. Rub, H. Bratzke, K. Del Tredici, Stages in the development of Parkinson's disease-related pathology, *Cell. Tissue Res.* 318 (2004) 121-134. doi: [10.1007/s00441-004-0956-9](https://doi.org/10.1007/s00441-004-0956-9).
- [37] L. Dahan, B. Astier, N. Vautrelle, N. Urbain, B. Kocsis, G. Chouvet, Prominent burst firing of dopaminergic neurons in the ventral tegmental area during paradoxical sleep, *Neuropsychopharmacology* 32 (2007) 1232-1241. doi: [10.1038/sj.npp.1301251](https://doi.org/10.1038/sj.npp.1301251).
- [38] M.M. Lima, M.L. Andersen, A.B. Roksidler, M.A. Vital, S. Tufik, The role of the substantia nigra pars compacta in regulating sleep patterns in rats, *PLoS One* 2 (2007) e513. doi: [10.1371/journal.pone.0000513](https://doi.org/10.1371/journal.pone.0000513).

[39] M.M. Lima, M.L. Andersen, A.B. Roksidler, A. Silva, A. Zager, S.M. Zanata, M.A. Vital, S. Tufik, Blockage of dopaminergic D(2) receptors produces decrease of REM but not of slow wave sleep in rats after REM sleep deprivation, *Behav. Brain Res.* 188 (2008) 406-411. doi: [10.1016/j.bbr.2007.11.025](https://doi.org/10.1016/j.bbr.2007.11.025).

[40] J. Mena-Segovia, J.P. Bolam, P.J. Magill, Pedunculo pontine nucleus and basal ganglia: distant relatives or part of the same family? *Trends. Neurosci.* 27 (2004) 585-588. doi: [10.1016/j.tins.2004.07.009](https://doi.org/10.1016/j.tins.2004.07.009).

[41] F. Mori, K.I. Okada, T. Nomura, Y. Kobayashi, The pedunculo pontine tegmental nucleus as a motor and cognitive interface between the cerebellum and basal ganglia. *Front. Neuroanat.* 10 (2016) 1-8. doi: [10.3389/fnana.2016.00109](https://doi.org/10.3389/fnana.2016.00109).

[42] S.B. Floresco, A.R. West, B. Ash, H. Moore, A.A. Grace, Afferent modulation of dopamine neuron firing differentially regulates tonic and phasic dopamine transmission, *Nat. Neurosci.* 6 (2003) 968-973. doi: [10.1038/nn1103](https://doi.org/10.1038/nn1103).

[43] G.L. Forster, C.D. Blaha, Pedunculo pontine tegmental stimulation evokes striatal dopamine efflux by activation of acetylcholine and glutamate receptors in the midbrain and pons of the rat, *Eur. J. Neurosci.* 17 (2003) 751-762. doi: [10.1046/j.1460-9568.2003.02511.x](https://doi.org/10.1046/j.1460-9568.2003.02511.x).

- [44] E. Garcia-Rill, C.R. Houser, R.D. Skinner, W. Smith, D.J. Woodward, Locomotion-inducing sites in the vicinity of the pedunculopontine nucleus, *Brain Res. Bull.* 18 (1987) 731-738. doi: [10.1016/0361-9230\(87\)90208-5](https://doi.org/10.1016/0361-9230(87)90208-5).
- [45] A.D. Targa, L.S. Rodrigues, A.C. Nosedá, M.F. Aurich, M.L. Andersen, S. Tufik, C. de Cunha, M.M. Lima, Unraveling a new circuitry for sleep regulation in Parkinson's disease, *Neuropharmacology* 108 (2016) 161-171. doi: [10.1016/j.neuropharm.2016.04.018](https://doi.org/10.1016/j.neuropharm.2016.04.018).
- [46] F. Vitale, C. Mattei, A. Capozzo, I. Pietrantonì, P. Mazzone, E. Scarnati, Cholinergic excitation from the pedunculopontine tegmental nucleus to the dentate nucleus in the rat, *Neuroscience* 317 (2016) 12-22. doi: [10.1016/j.neuroscience.2015.12.055](https://doi.org/10.1016/j.neuroscience.2015.12.055).
- [47] J. Mena-Segovia, H.M. Sims, P.J. Magill, J.P. Bolam, Cholinergic brainstem neurons modulate cortical gamma activity during slow oscillations, *J. Physiol.* 586 (2008) 2947-2960. doi: [10.1113/jphysiol.2008.153874](https://doi.org/10.1113/jphysiol.2008.153874).
- [48] D. Dautan, I. Huerta-Ocampo, I.B. Witten, K. Deisseroth, J.P. Bolam, T. Gerdjikov, J. Mena-Segovia, A major external source of cholinergic innervation of the striatum and nucleus accumbens originates in the brainstem, *J. Neurosci.* 34 (2014) 4509-4518. doi: [10.1523/JNEUROSCI.5071-13.2014](https://doi.org/10.1523/JNEUROSCI.5071-13.2014).
- [49] J.L. Lanciego, N. Luquin, J.A. Obeso, Functional neuroanatomy of the basal ganglia, *Cold Spring Harb. Perspect. Med.* 2 (2012) a00962. doi: [10.1101/cshperspect.a009621](https://doi.org/10.1101/cshperspect.a009621).

[50] S. Perez-Lloret, F.J. Barrantes, Deficit of cholinergic neurotransmission and their clinical correlates in Parkinson's disease, *npj Parkinson's Disease* 2 (2016) 16001. doi: [10.1038/npjparkd.2016.1](https://doi.org/10.1038/npjparkd.2016.1).

[51] K.C. Andrade, V.I. Spoormaker, M. Dresler, R. Wehrle, F. Holsboer, P.G. Samann, M. Czisch, Sleep spindles and hippocampal functional connectivity in human NREM sleep, *J. Neurosci.* 31(2011) 10331-10339. doi: [10.1523/JNEUROSCI.5660-10.2011](https://doi.org/10.1523/JNEUROSCI.5660-10.2011).

[52] Y. Urakami, A.A. Ioannides, G.K. Kostopoulos, Sleep Spindles – As a Biomarker of Brain Function and Plasticity, in: I.M. Ajeena, (Eds.) *Advances in Clinical Neurophysiology*, InTech, Rijeka, Croatia, 2012, pp. 73-108. doi: [10.5772/48427](https://doi.org/10.5772/48427).

[53] L. Graves, A. Pack, T. Abel, Sleep and memory: a molecular perspective. *Trends Neurosci.* 24 (2001) 237-243. doi: [10.1016/S0166-2236\(00\)01744-6](https://doi.org/10.1016/S0166-2236(00)01744-6).

[54] D. Sullivan, K. Mizuseki, A. Sorigi, G. Buzsaki, Comparison of sleep spindles and theta oscillations in the hippocampus, *J. Neurosci.* 34 (2014) 662-674. doi: [10.1523/JNEUROSCI.0552-13.2014](https://doi.org/10.1523/JNEUROSCI.0552-13.2014).

[55] A. Quiroga-Varela, J.R. Walters, E. Brazhnik, C. Marin, J.A. Obeso, What basal ganglia changes underlie the parkinsonian state? The significance of neuronal oscillatory activity, *Neurobiol. Dis.* 58 (2013) 242-248. doi: [10.1016/j.nbd.2013.05.010](https://doi.org/10.1016/j.nbd.2013.05.010).

[56] S. Ge, C. Yang, M. Li, J. Li, X. Chang, J. Fu, L. Chen, C. Chang, X. Wang, J. Zhu, G. Gao, Dopamine depletion increases the power and coherence of high-voltage spindles in the globus pallidus and motor cortex of freely moving rats, *Brain Res.* 1465 (2012) 66-79. doi: [10.1016/j.brainres.2012.05.002](https://doi.org/10.1016/j.brainres.2012.05.002).

ACCEPTED MANUSCRIPT

Figures Legends

Fig. 1. Typical examples of the final scatter-grams of Wake/NREM/REM states (W/NR/R; black dots/black circles/black crosses) differentiation, simultaneously recorded from the motor cortex (MCx) and hippocampus (Hipp) during 6 h of normal inactive circadian phase for rats (overall 2160 10 s Fourier epochs), with the extracted simultaneous (common) Wake/NREM/REM 10 epochs (Wc/NRc/Rc; red dots/blue circles/green crosses) within the MCx and Hipp of control rat (Control-i).

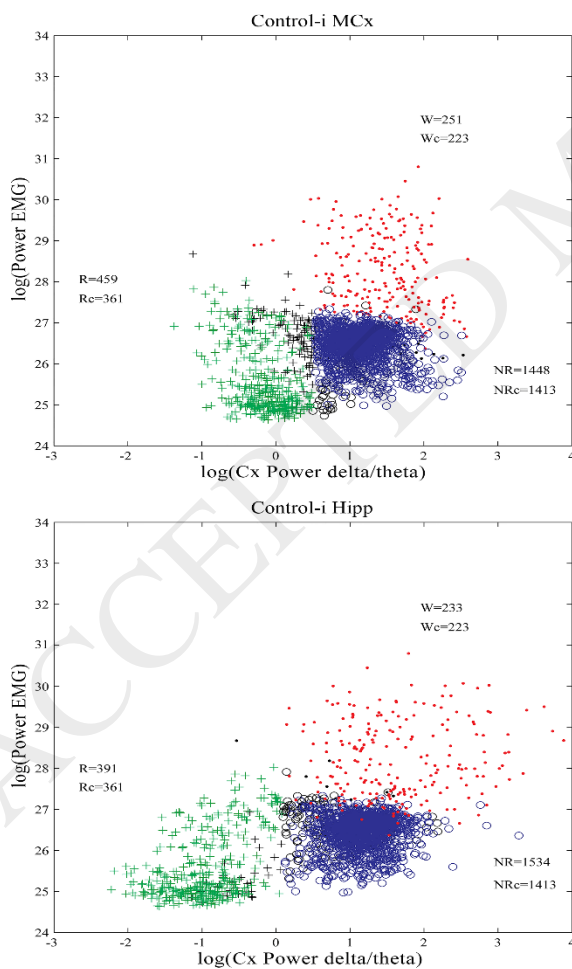
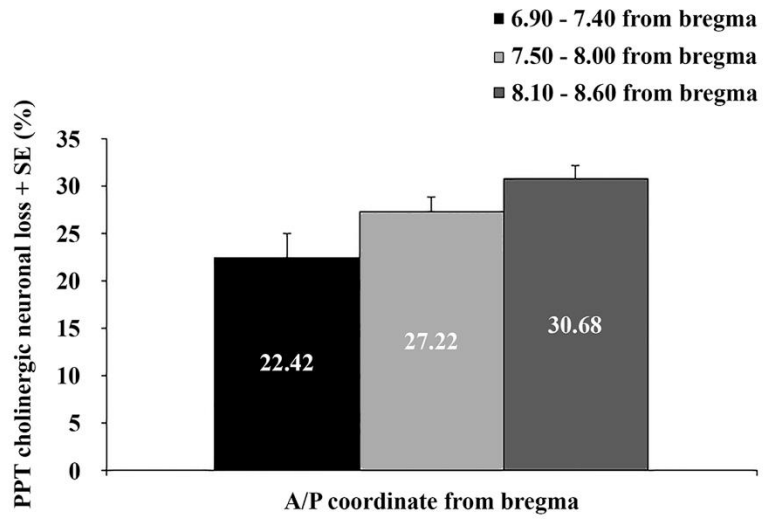


Fig. 2. Histological identification and quantification of the bilateral cholinergic neuronal loss throughout the overall rostro-caudal dimension of the PPT (from 6.90 to 8.60 mm caudally from bregma), counted in three stereotaxic ranges (6.90-7.40; 7.50-8.00; and 8.10-8.60 mm caudally from bregma) per each brain side (n = 11 for controls; n = 11 for the PPT lesion). The mean cholinergic neuronal loss was > 22 % throughout the overall PPT dimension on each brain side, with the maximal loss caudally of 30.68 ± 6.28 % (**A**). Typical example of the histological identification of PPT lesion by NADPH - diaphorase staining (**B**) in three brain sections (right panels) vs. control brain (Control-i brain, left panels) that represents each stereotaxic range for the group means calculation of the cholinergic neuronal loss per each brain side.

In this PPT lesioned rat the cholinergic neuronal loss on this brain side was 31.81 % at 7.40 mm caudally from bregma, 33.33 % at 8.00 mm caudally from bregma, and 39.93 % at 8.30 mm caudally from bregma. PPT – pedunculopontine tegmental nucleus; xscp – decussation of the superior cerebellar peduncle; MnR – median raphe nucleus; LDT – laterodorsal tegmental nucleus; Black stars mark the lesioned PPT; Scale bar 200 μ m for all panels.

A



B

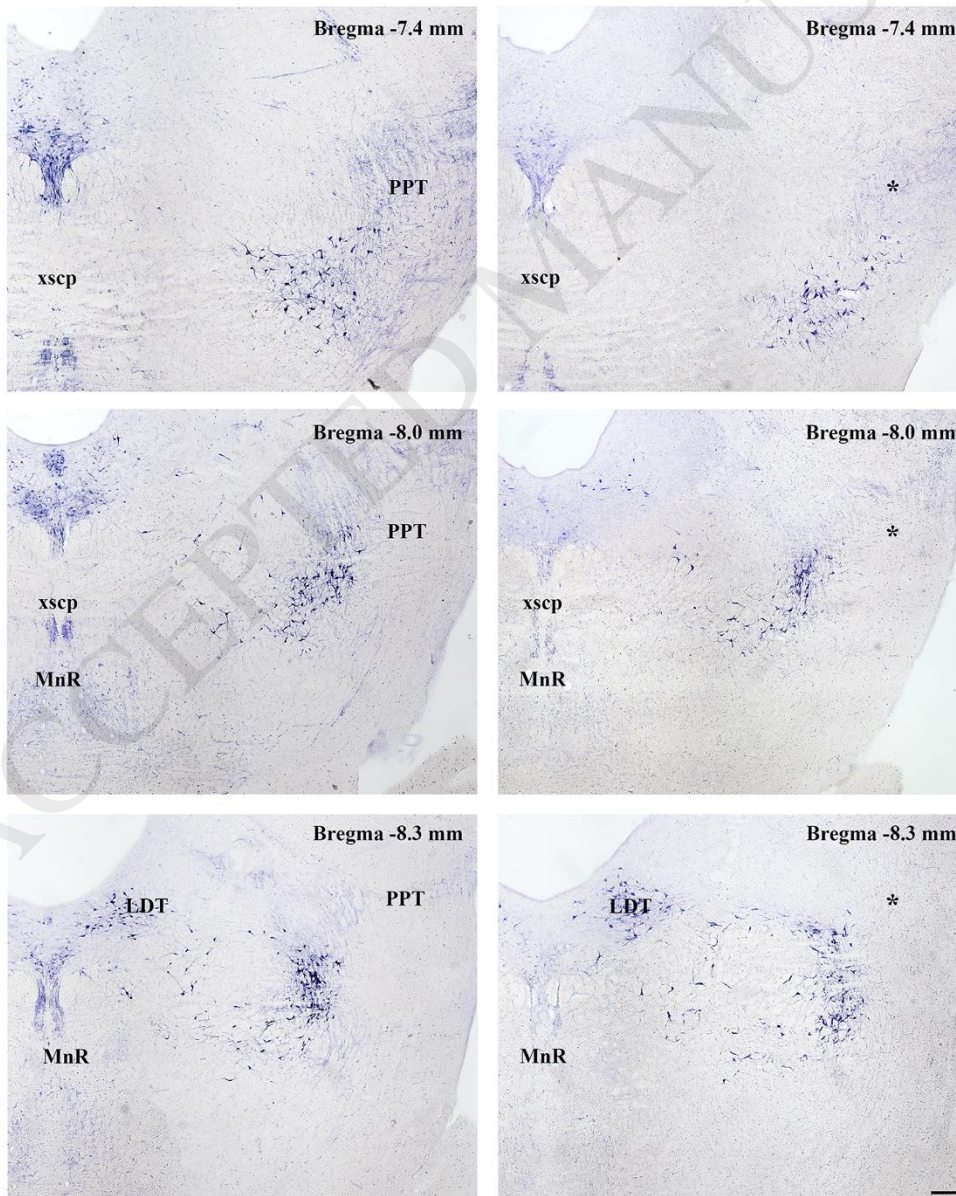
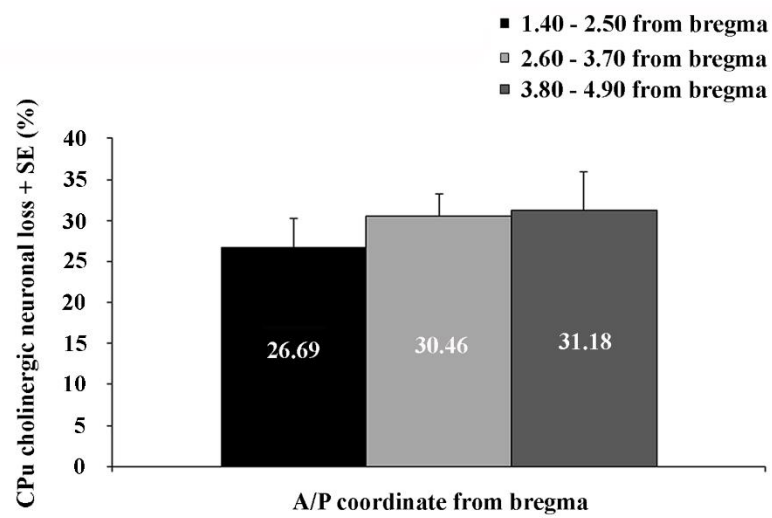


Fig. 3. Histological identification and quantification of the remote cholinergic neuronal loss in the caudate putamen (from 1.40 to 4.90 mm caudally from bregma), following the bilateral PPT lesion, counted in three stereotaxic ranges (1.40-2.50; 2.60-3.70; and 3.80-4.90 mm caudally from bregma) per each brain side (n = 6 for the controls; n = 8 for the PPT lesion). The mean cholinergic neuronal loss in the caudate putamen was also > 26 % throughout its overall rostro-caudal dimension per each brain side, with the maximal cholinergic neuronal loss within the most caudal stereotaxic range of 31.18 ± 14.13 % (**A**). Typical example of the identified remote cholinergic neuronal loss in the caudate putamen by NADPH - diaphorase staining (**B**) in three brain sections (bottom panels) vs. control brain (Control-i brain, upper panels) that presents each stereotaxic range for the group means calculation of the cholinergic neuronal loss per each brain side. In this individual example of the PPT lesioned rat, the remote cholinergic neuronal loss on this brain side was 35.45 % at 1.99 mm caudally from bregma, 40.66 % at 2.91 mm caudally from bregma, and 54.48 % at 3.84 mm caudally from bregma. CPu – caudate putamen; GP – globus pallidus; Black stars mark the lesioned caudate putamen. Scale bar 200 μ m for all panels.

A



B

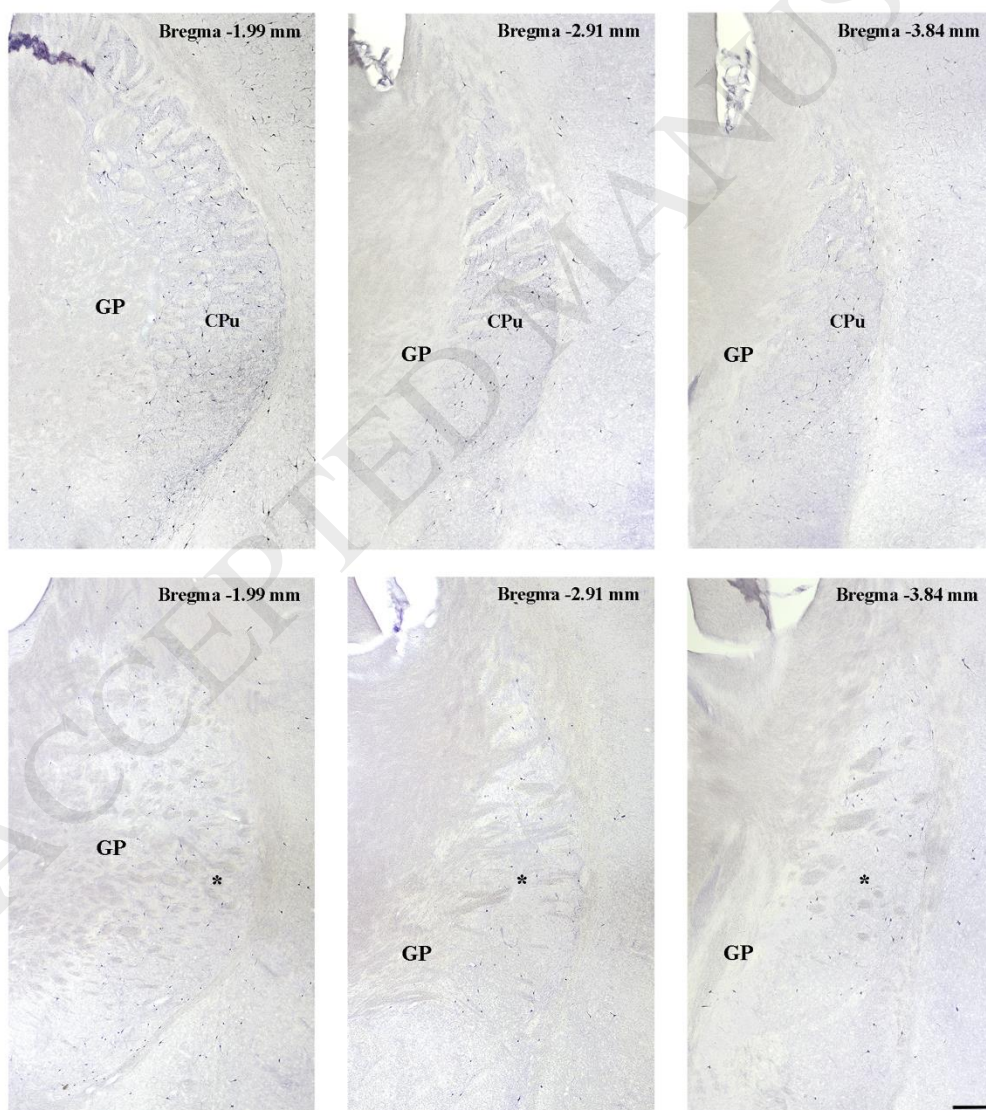


Fig. 4. Alteration of the spontaneous locomotor activity 14, 42, and 91 days following the PPT lesion. The data are expressed as the means for 5 min intervals (left panels) or as the means \pm SE for 30 min intervals (right panels). Time-dependent profiles of locomotor activity (left panels) were similar for all experimental groups (the physiological controls (Control-p), $n = 7$; the implanted controls (Control-i), $n = 7$; the PPT lesioned rats (PPT lesion), $n = 7$); but with evidently diminished locomotor activity in all time points from 42 to 91 days following the PPT lesion. Importantly, the locomotor activity score for the entire registration period (right panels) was significantly lower in the PPT lesioned group vs. Control-p and Control-i groups from 42 to 91 days after the PPT lesion. There were no significant differences between Control-p and Control-i groups. *# $p < 0.05$.

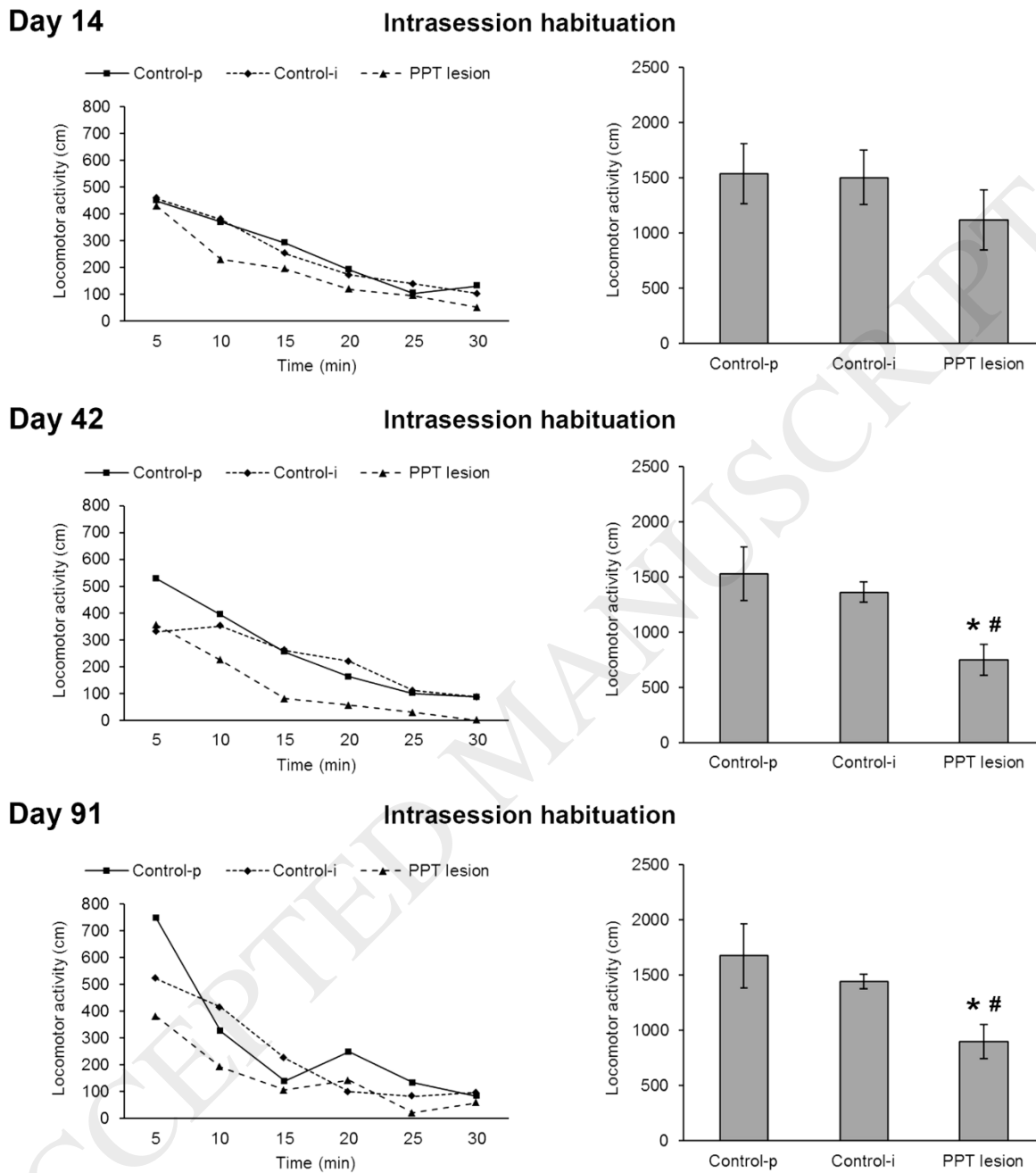


Fig. 5. EEG microstructure during NREM sleep in the hippocampus from 14 to 91 days following the bilateral PPT lesion. Group probability density distribution/6 h of the EEG delta, theta, sigma and beta relative amplitudes during simultaneous NREM sleep in the hippocampus (Hipp) and motor cortex (MCx) of the PPT lesioned rats (n = 10) vs. Control-i rats (n = 9).

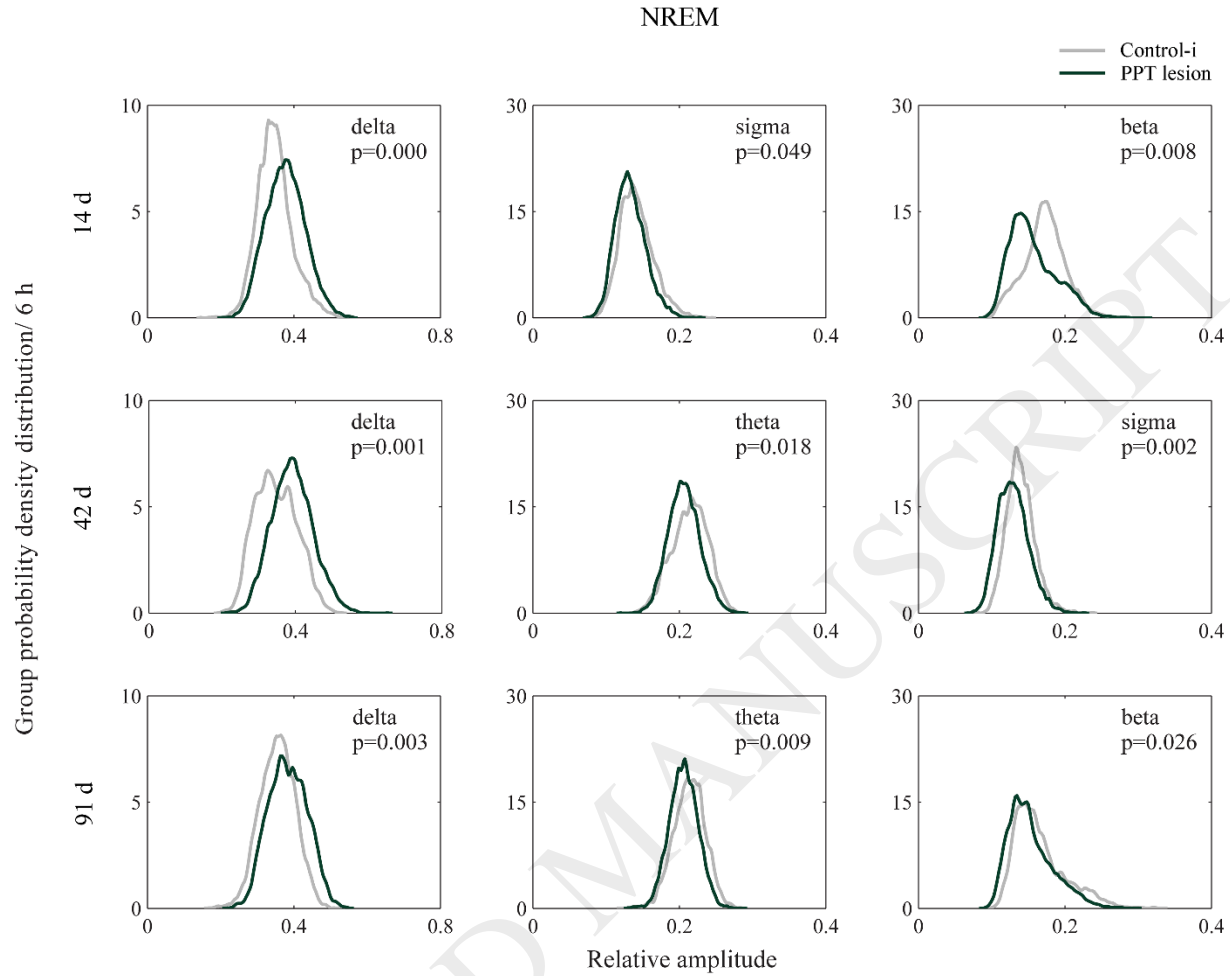


Fig. 6. EEG microstructure during simultaneous NREM sleep in the hippocampus and motor cortex 91 days following the bilateral PPT lesion. Group probability density distribution/6 h of the EEG delta, theta, beta and gamma relative amplitudes during simultaneous NREM sleep in the motor cortex (MCx) and hippocampus (Hipp) of the PPT lesioned rats ($n = 6$) vs. Control-i rats ($n = 5$).

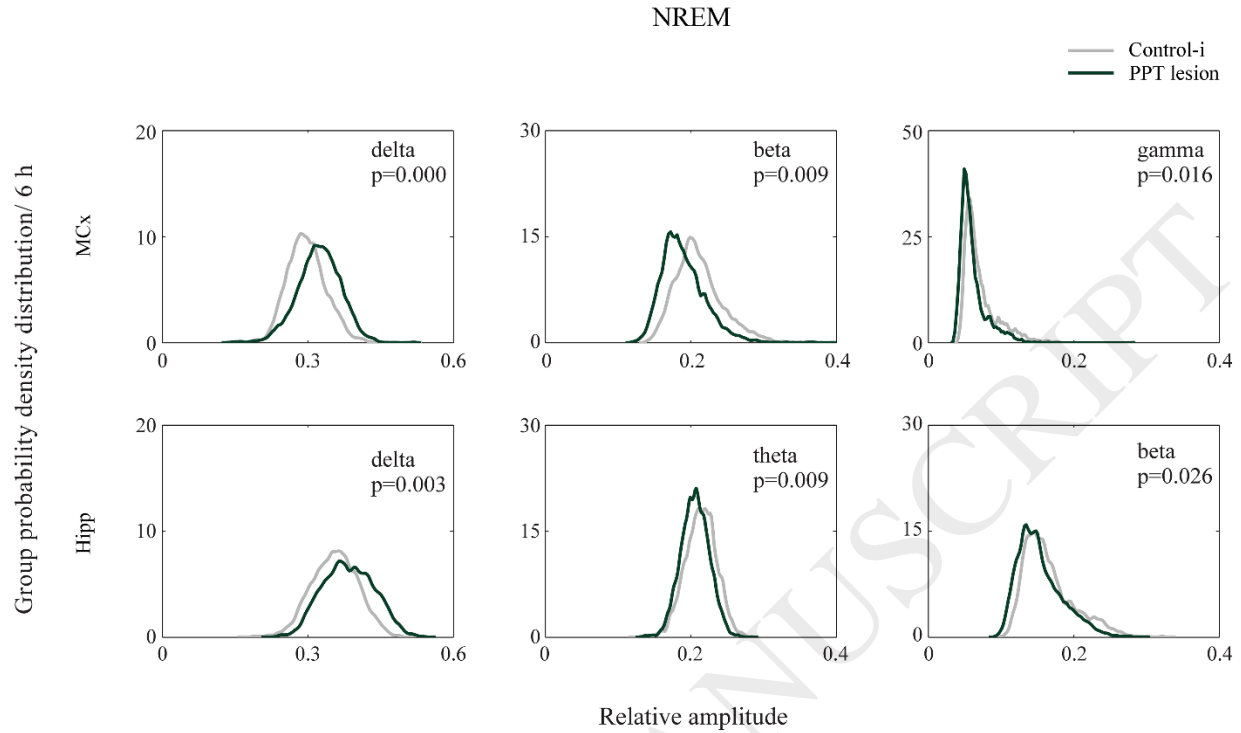


Fig. 7. Group probability density distributions of the EEG expanded theta relative amplitudes (4.1 – 10 Hz) during simultaneous REM sleep of the motor cortex (MCx) and hippocampus (Hipp). This approach enable us to detect the simultaneously augmented expanded theta amplitude due to an increased occurrence of the high voltage spindles (HVS) from 42 days following the PPT lesion ($n = 9$) vs. Control-i rats ($n = 8$) during REM of both brain structures, but 91 days after the lesion only during REM within the MCx.

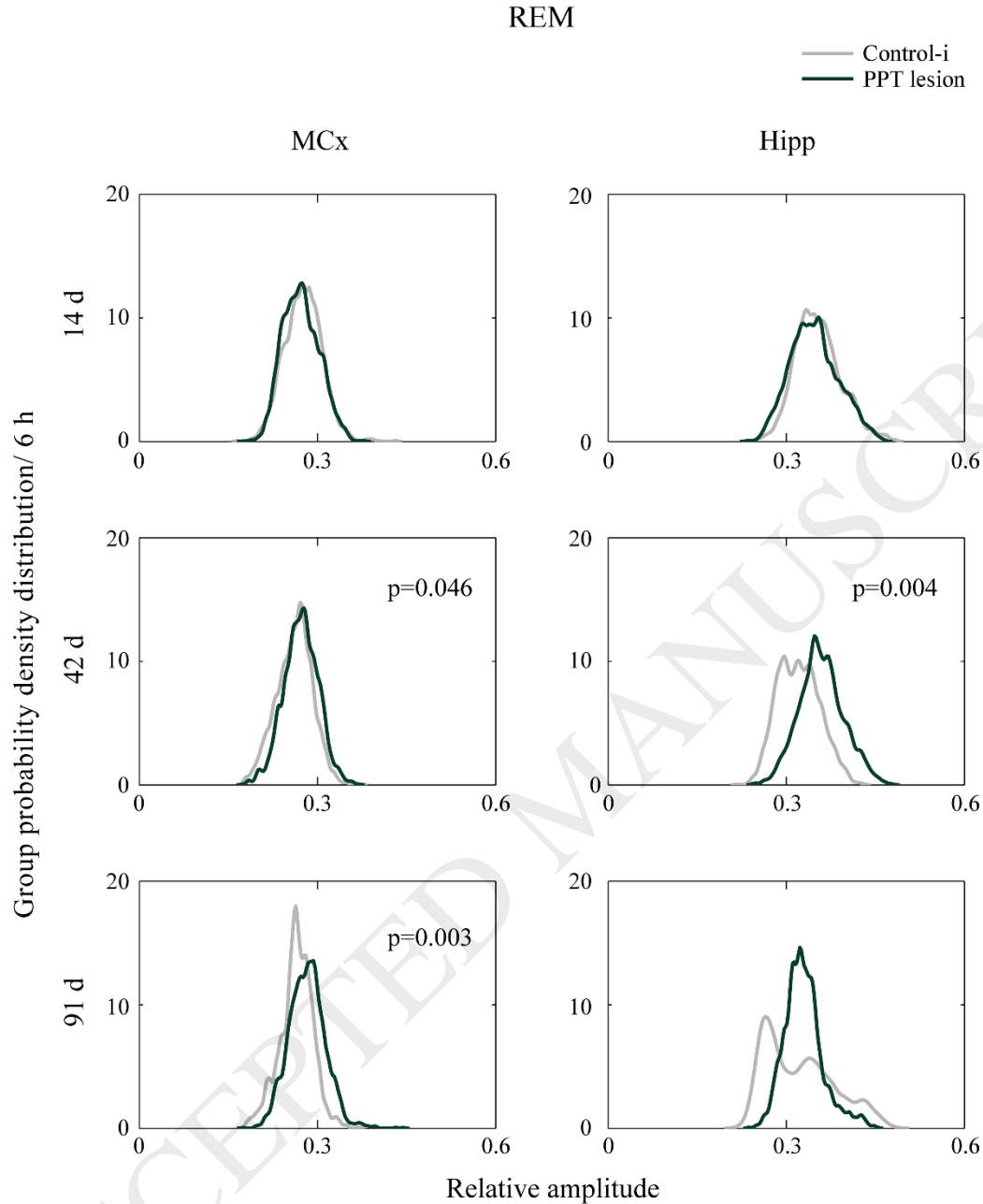


Fig. 8. Impact of the bilateral PPT lesion on the high voltage spindles (HVS) duration and intrinsic frequency during the simultaneous REM sleep of the motor cortex (MCx) and hippocampus (Hipp) and across the overall sleep follow-up period (from 14 to 91 days after the PPT lesion). Whereas the probability density distributions included 414 HVS from MCx and 248 HVS from Hipp of the Control-i rats (grey distributions), they included 1338 HVS from MCx

and 1449 HVS from Hipp of the PPT lesioned rats (black distributions) during the simultaneous REM sleep of both structures. Whereas the PPT lesion generally increased the HVS frequency/6 h during the simultaneous REM sleep of the MCx and Hipp (see **Table 1**), it prolonged the HVS duration (**A**, bottom left panel, right shifted black distribution) without change in the intrinsic frequency (**A**, bottom right panel) only in the MCx, but decreased the HVS duration (**B**, left bottom panel; left shifted black distribution) and intrinsic frequency (**B**, right bottom panel; left shifted black distribution) in the Hipp. The individual example of 30 s analog signals with the HVS from MCx (**A**) and Hipp (**B**) during REM sleep depicts the probability density group data of the HVS duration and intrinsic frequency (**A**, **B** three upper panels).

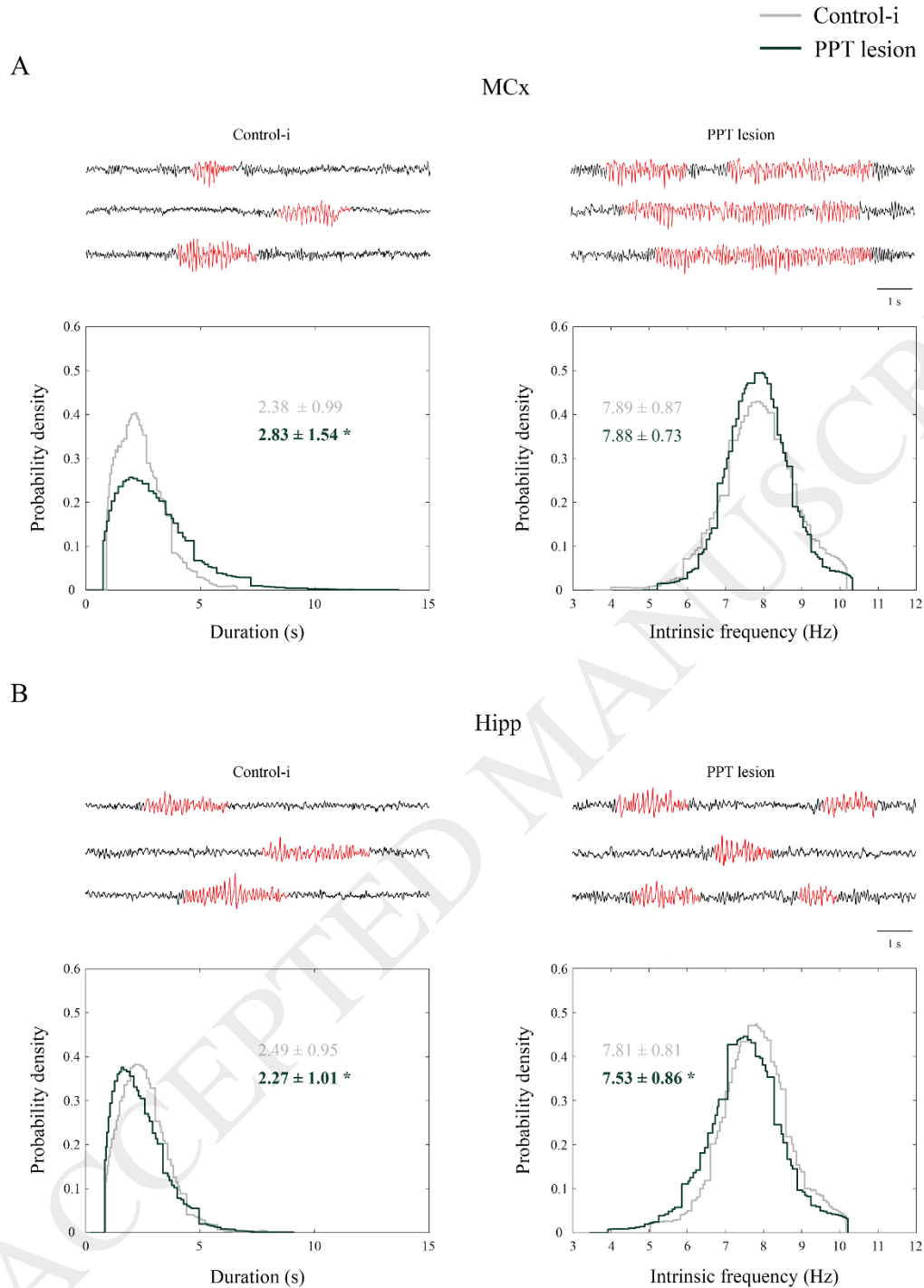
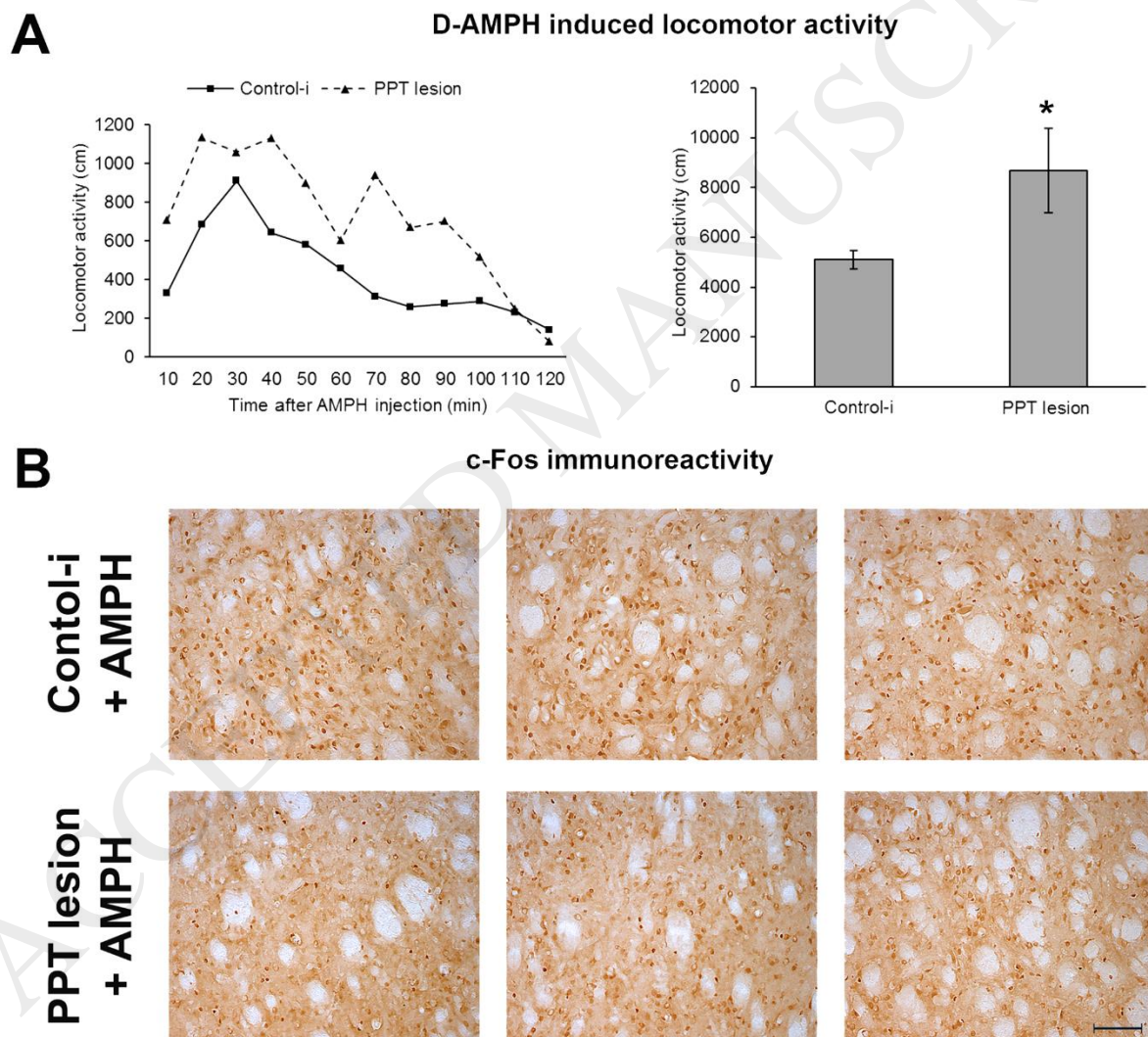


Fig. 9. Effect of amphetamine on locomotor activity and c-Fos immunostaining within the caudate putamen 91 days after the PPT lesion. D-amphetamine-induced hyperactivity was expressed as the mean values for 10 min intervals (upper left panel) or as the mean \pm SE for 120

min registration period (upper right panel). Note that the PPT lesion group ($n = 5$) compared to the control group ($n = 7$) showed hyperactivity in all time points from 10 to 110 min of registration period (**A**, left panel), resulting in significantly higher total locomotor activity score (**A**, right panel). Representative photomicrographs of c-Fos-positive cells in the caudate putamen (**B**; c-Fos immunostaining) following amphetamine injections in 3 Control-i rats (**B**, upper panels) vs. 3 PPT lesioned rats (**B**, lower panels). $*p < 0.05$; Scale bar 50 μm for all panels.



Table

Table 1. High voltage sleep spindles (HVS) density, their mean duration and intrinsic frequency \pm SD during common REM sleep of the motor cortex (MCx) and hippocampus (Hipp) per 6 h of sleep recording, and across the overall sleep follow-up period after the bilateral PPT lesion (from 14 to 91 days after the PPT lesion) vs. controls (Controls-i). Bold numbers and asterisks indicate the statistically significant mean values at $p \leq 0.05$. In addition, the asterisks indicate the statistically significant means for HVS density, duration and intrinsic frequency between MCx and Hipp (distinct inter-structural HVS dynamic) in the Control-i vs. the PPT lesioned rats.

	MCx			Hipp		
	Density/6h	Duration/6h (s)	Frequency/6h (Hz)	Density/6h	Duration/6h (s)	Frequency/6h (Hz)
14 d						
Control-i	0.007 \pm 0.003	2.43 \pm 1.03	8.02 \pm 0.78	0.004 \pm 0.002	2.55 \pm 0.97	7.82 \pm 0.78*
PPT lesion	0.017 \pm 0.006	2.76 \pm 1.36	7.76 \pm 0.70	0.015 \pm 0.006	2.35 \pm 1.01*	7.50 \pm 0.79*
42 d						
Control-i	0.013 \pm 0.006	2.33 \pm 0.94	7.53 \pm 0.90	0.011 \pm 0.006*	2.40 \pm 1.10	7.59 \pm 0.78

PPT lesion	0.026 ± 0.012	2.68 ± 1.46	7.93 ± 0.79	0.017 ± 0.009	2.18 ± 0.99*	7.48 ± 0.91*
<i>91 d</i>						
Control-i	0.005 ± 0.002	2.39 ± 0.96	8.05 ± 0.90	0.002 ± 0.002	2.50 ± 0.87	8.12 ± 0.86
PPT lesion	0.027 ± 0.009	2.97 ± 1.70	7.94 ± 0.70	0.029 ± 0.011	2.26 ± 1.02*	7.59 ± 0.88*

Bold numbers indicate the statistically significant mean values at $p \leq 0.05$.

Asterisks indicate the statistically significant inter-structure mean values at $p \leq 0.05$.